Cumhuriyet Science Journal
CSJ

e-ISSN: 2587-246X
ISSN: 2587-2680

Cumhuriyet Sci. J., Vol.40-3 (2019) 583-594

A Mechanism of Eddy Generation in A Single Lid-Driven T-Shaped Cavity

Ebutalib ÇELİK [1], ***Ali DELİCEOĞLU*** [1,*]

[1] *Department of Mathematics, Science Faculty, Erciyes University, Kayseri 38039, TURKEY*

Received: 24.05.2019; Accepted: 15.08.2019 *http://dx.doi.org/10.17776/csj.569655*

Abstract. The two-dimensional (2D) steady, incompressible, Stokes flow is considered in a T-shaped cavity which has the upper-lid moving in horizontal directions. A Galerkin finite element method is used to investigate a new eddy generation and flow bifurcation. The flow in a cavity is controlled by two parameters h_1 and h_2 which are associated with the heights of the T-shaped domain. By varying h_1 and h_2, the second eddy formation mechanism and the h_1, h_2 control space diagram are obtained.

Keywords**:** A T-shaped cavity, Stokes flow, eddy generation

Tek Kapağı Sürgülü T-Şeklindeki Kaviti İçerisindeki Girdap Oluşum Mekanizması

Özet. Üst kapağı yatay yönde hareket eden T şeklindeki kaviti içerisindeki iki boyutlu (2D) durağan, sıkıştırılamaz, Stokes akış ele alındı. Yeni girdap oluşumunu ve akış çatallanmasını araştırmak için Galerkin sonlu elemanlar yöntemi kullanıldı. Kaviti içersindeki akış, T-şeklindeki bölgenin h_1 ve h_2 yükseklik parametreleri tarafından kotrol edilir. h_1 ve h_2 yüksekliklerinin değişmesiyle meydana gelen girdap oluşum mekanizması ve h_1, h_2 kontrol uzay diyagramı elde edildi.

Anahtar Kelimeler**:** T-şekilli kaviti, Stokes akış, girdap oluşumu

1. INTRODUCTION

Stokes flow within the closed domain has always been an interesting area of study in computational fluid dynamics. Thanks to the simplicity of the geometric shapes and the easy installation of the related boundary value problem, a lot of work has been done about the driven cavity [1- 8]. In addition, cavity problems are considered as an application of theoretical studies on the investigation of the qualitative properties of streamlines, which is a subject of fluid dynamics [9-12].

In the literature, there are many studies on the flow of square lid-driven cavity flow both numerically and theoretically [13-18]. Gürcan [19] investigated the flow problem of the rectangular cavity with both a single lid-driven and a double lid-driven and examined the vortex formation mechanism in the cavity. He used the analytical solution of the streamfunction expanded about any critical point in the cavity. The control space diagram (S, A) including the aspect ratio A and the velocity ratio S was obtained and investigated the effect of the changes in the ratio of A on vortex formation.

* Corresponding author. *Email address:* *adelice@erciyes.edu.tr*

In addition to the square and rectangular domain commonly used in cavity flow problems, different closed domain are also studied. To investigate the effect of cavity geometry on the flow structure, McQuain [20] studied steady, viscous flow within the square, trapezoidal and triangular cavity. Gaskell [21] considered Stokes flow within the half-filled annulus between rotating coaxial cylinders and showed that changes in flow structure arose directly from stagnation point where a saddle point transformed into a centre and vice versa. The 2-D steady, incompressible flow inside a triangular driven cavity is considered numerically in papers of [6, 22, 23]. Gürcan and Bilgil [24] have obtained the vortex formation mechanism in the sectoral cavity as the A aspect ratio decreases for different lid speed ratio. They formed control space diagram with controller parameters A ∈ (1.6,1.65) and S ∈ [−1,0] which is consisted of the curves representing the flow bifurcation at critical points. Finally, they [25] investigated the effect of Reynolds number on the flow bifurcation and vortex formation on the same domain.

Recently, Deliceoğlu and Aydın [26] have considered the flow problem in a L-shaped cavity which has the lids moving in the opposite direction using the numerical method. They have obtained solutions of the Stokes and the Navier-Stokes equations that govern the flow inside the domain using the Galerkin finite element method. Further, they obtained h_1, h_2 control space diagram for the L-shaped cavity with the height of the lower part h_1 and of the upper part h_2. It was determined how this diagram changed when the Reynolds number was 500. In the continuation of their study [7], they have obtained analytical solutions for the Stokes equation for the steady, viscous and single lid-driven flow on the same region. The flow patterns obtained within the region depending on the heights of h_1 and h_2.

To our knowledge, there is no study on the lid-driven cavity flow inside the T-shaped closed domain in the literature. Unlike other regions, the T-shaped cavity has two symmetrical re-entrant corner points. In this paper, we assume that the flow inside the domain is steady, viscous and incompressible. By changing the heights of the lower and of the upper part of the cavity, flow patterns within the region are obtained and the vortex formation mechanism in the parameter space h_1, h_2 is presented.

2. PROBLEM SPECIFICATION AND FORMULATION

We will consider the fluid flow in a two-dimensional upper lid-driven T-shaped cavity with rigid walls as shown in Figure 1. It is assumed that the fluid is Newtonian and incompressible with density ρ and viscosity μ. The flow is steady and two dimensional in the (x, y) plane with velocity u = (u, v). In non-dimensional form, the width of the cavity is fixed (L = 6), the height of the lower part and upper part, called h_1 and h_2, are varying, then the flow topology is determined.

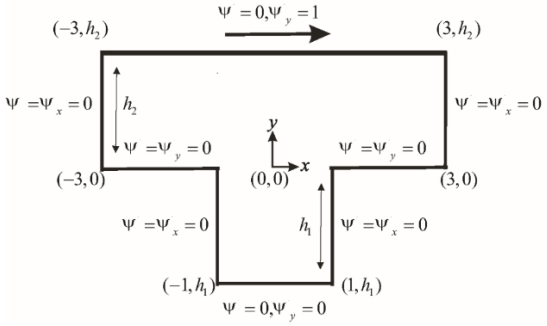

Figure 1: Boundary conditions for the lid-driven T-shaped cavity.

In this paper, it will be concerned that the fluid is steady, incompressible viscous flow. The equation governing the flow field along the cavity is the Stokes equation as the follows:

$$\begin{cases} -\dfrac{1}{\mathrm{Re}}\Delta\mathbf{u}+\nabla p = f \quad \text{in} \quad \Omega, \\ \nabla\cdot\mathbf{u}=0 \qquad\quad \text{in} \quad \Omega. \end{cases} \tag{1}$$

If we assume that the external force is negligible so f is zero, then the equation can be written in terms of stream function as follows,

$$\begin{cases} \nabla^4\psi(x,y)=\left(\dfrac{\partial^4}{\partial x^4}+2\dfrac{\partial^4}{\partial x^2\partial y^2}+\dfrac{\partial^4}{\partial y^4}\right)\psi(x,y)=0, \\ \psi=\text{constant}, \dfrac{\partial\psi}{\partial n}=\text{constant}. \end{cases} \tag{2}$$

The weak formulation of (2) can be written by [27] as follows: find $\Psi\in V=H_0^2(\Omega)$ such that

$$B(\Psi,\Phi)=(\Delta\Psi,\Delta\Phi)=\int_\Omega \Delta\Psi\Delta\Phi d\Omega=0 \tag{3}$$

for all $\Phi\in H_0^2(\Omega)$ where H_0^2 is the class of all H^2 functions satisfying the boundary condition of (2) and Δ is the Laplacian operator. In this study, the standard Galerkin finite element method is used to solve the bi-harmonic problem (2). In this method, approximation of the problem is determined by the choice of finite dimensional subspace $V_h\subset V$ defined on a family of regular quadrangular discretizations T_h of the domain. A bicubic quadrangular elements are choosed to apply the finite element method as

$$B(\Psi_h,\Phi_h)=(\Delta\Psi_h,\Delta\Phi_h)=0 \quad \forall(\Psi_h,\Phi_h)\in V_h .$$

Since the test function $\Psi_h\in H^2$, it follows that the basis function Φ_h have continuous first partial derivatives across the boundaries. These provide a two-dimensional version of Hermite interpolation functions as a basis function on a rectangular element. They are constructed by substituting the product of a cubic equation in x by a cubic in y resulting a collection of 16 monomials

$$\begin{bmatrix} 1 \\ x \\ x^2 \\ x^3 \end{bmatrix}\begin{bmatrix} 1 & y & y^2 & y^3 \end{bmatrix}=\begin{bmatrix} 1 & y & y^2 & y^3 \\ x & xy & xy^2 & xy^3 \\ x^2 & x^2y & x^2y^2 & x^2y^3 \\ x^3 & x^3y & x^3y^2 & x^3y^3 \end{bmatrix}$$

For each element, the coefficient of these monomials are calculated using each of the following four quantities:

$$\left\{\Psi_h,\frac{\partial\Psi_h}{\partial x},\frac{\partial\Psi_h}{\partial y},\frac{\partial^2\Psi_h}{\partial x\partial y}\right\},$$

at each corner of the rectangle. See [27,28] for more information.

3. FLOW STRUCTURES IN THE T-SHAPED CAVITY

In this section, we will show a flow structures topologically occurring and describe the vortex formation within the T-shaped cavity as the varying of the heights of the lower part h_1 and the upper part h_2. By changing of these parameters, bifurcation curves are obtained to reveal changes in the flow structure. Here, the expression of the change in the flow structure refers to the transformation of the type of stationary point from the saddle to the center or vice versa. The (h_1, h_2) parameter space is obtained by finding the critical values of h_1 and h_2 in which structural changes occur.

We consider (h_1, h_2) parameter space in the interval between $-3.5 < h_1 < -0.2$ and $0.2 < h_2 < 10.5$, so we have obtained a 23 different flow topologies shown by Figure 2, Figure 3 and Figure 4. A set of co-dimension-one bifurcation curves in the parameter space are obtained by using the numerical methods. The co-dimension of a bifurcation is the smallest number of parameters needed to find bifurcation. The control-space diagram is formed by fixing h_1 while changing h_2 or vice versa. Then, the related bifurcation curves are illustrated in Figure 5.

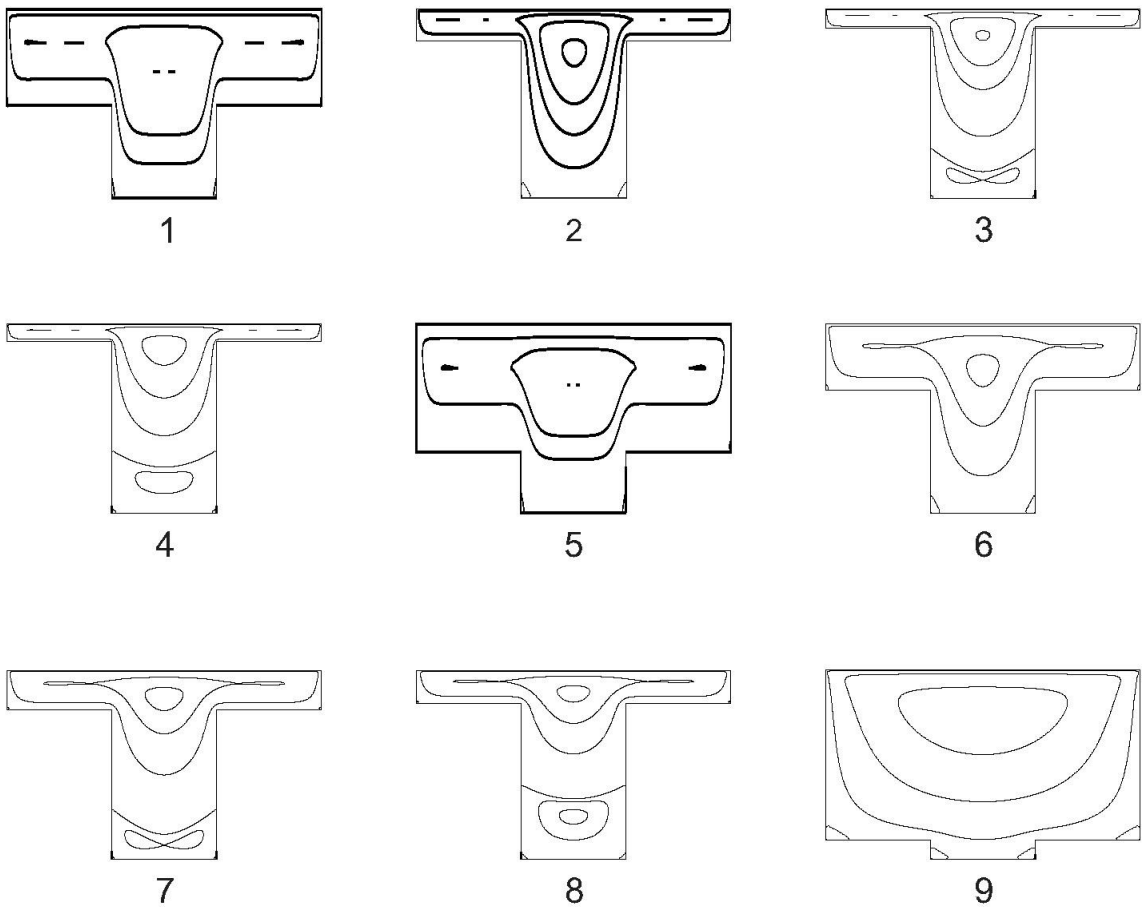

Figure 2. *Representation of the flow patterns within the domain: (1)* h_1 *= -0.29,* h_2 *= 0.3, (2)* h_1 *= -1.75,* h_2 *= 0.35, (3)* h_1 *= -3.1,* h_2 *= 0.35, (4)* h_1 *= -3.4,* h_2 *= 0.35, (5)* h_1 *= -0.205,* h_2 *= 0.42, (6)* h_1 *= -1.3,* h_2 *= 0.7, 7)* h_1 *=-0.64,* h_2 *= 0.7, (8)* h_1 *= -3.3,* h_2 *= 0.7, (9)* h_1 *= -0.6,* h_2 *=5.45.*

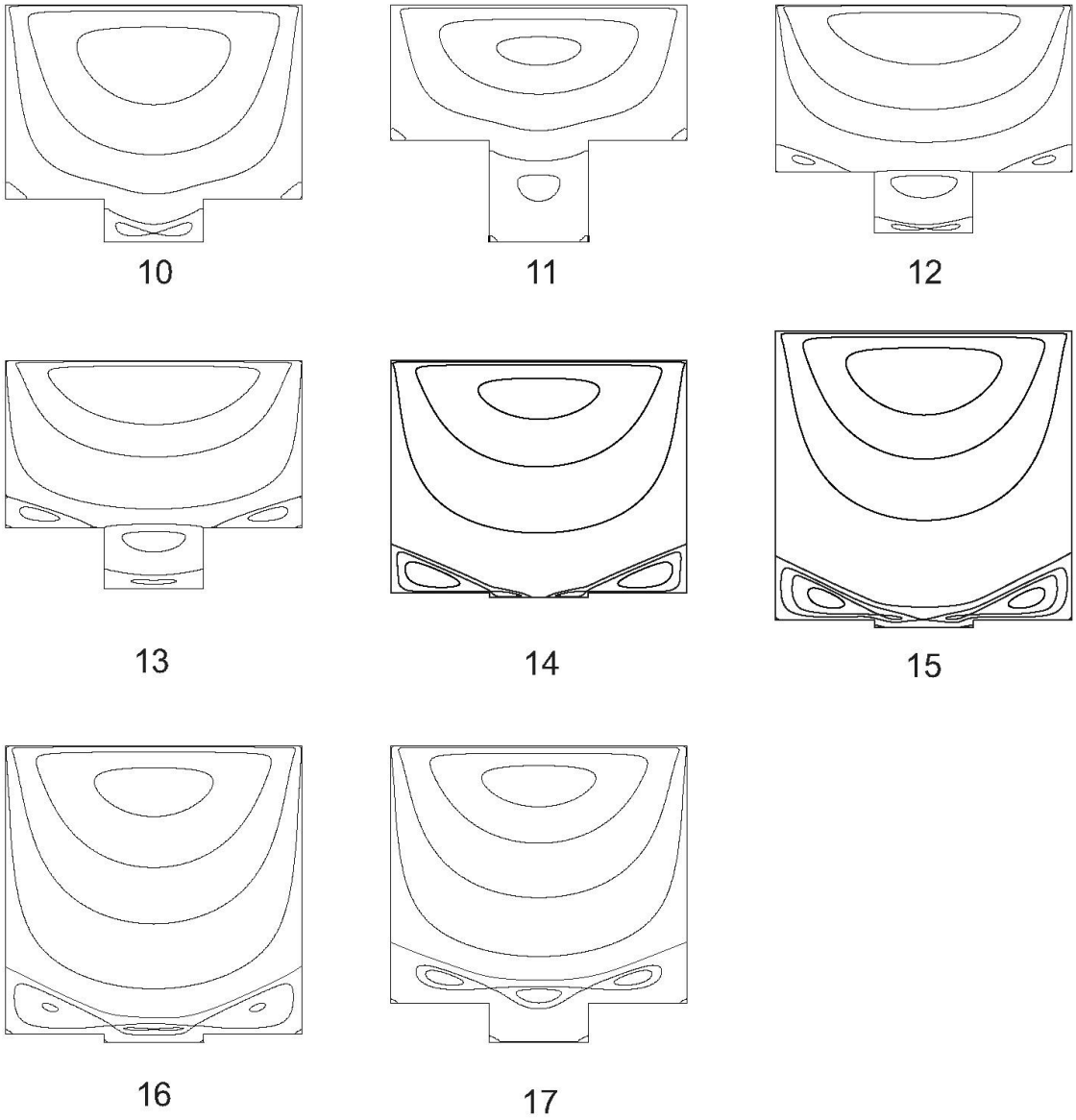

Figure 3. *Representation of the flow patterns within the domain (continued): (10)* h_1 *= -1.1,* h_2 *= 4.95, (11)* h_1 *= ---2.6,* h_2 *= 3.45, (12)* h_1 *= -3.4,* h_2 *= 9.3, (13)* h_1 *= -3.47,* h_2 *= 9.5, (14)* h_1 *= -0.2,* h_2 *= 9.605, (15)* h_1 *= -0.23,* h_2 *= 9.7, (16)* h_1 *= -0.28,* h_2 *= 9.75, (17)* h_1 *= -1.5,* h_2 *= 9.9.*

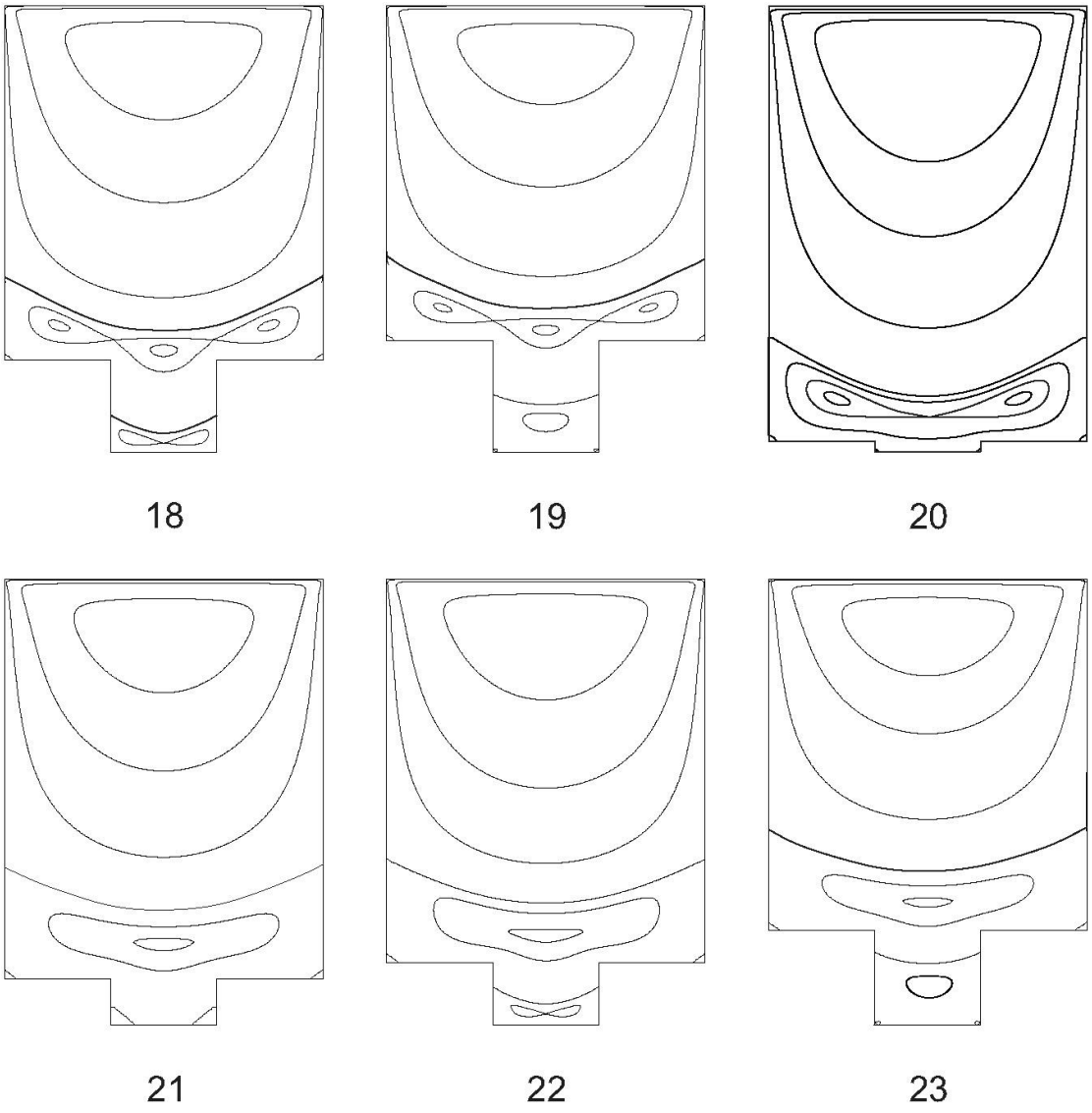

Figure 4. *Representation of the flow patterns within the domain (continued): (18)* h_1 *= -2.57,* h_2 *= 9.87,(19)* h_1 *= --3.3,* h_2 *= 9.9, (20)* h_1 *= -0.23,* h_2 *= 10.1, (21)* h_1 *= -1.2,* h_2 *= 10.4, (22)* h_1 *= -1.7,* h_2 *= 10.4, (23)* h_1 *= -2.8,* h_2 *= 10.4.*

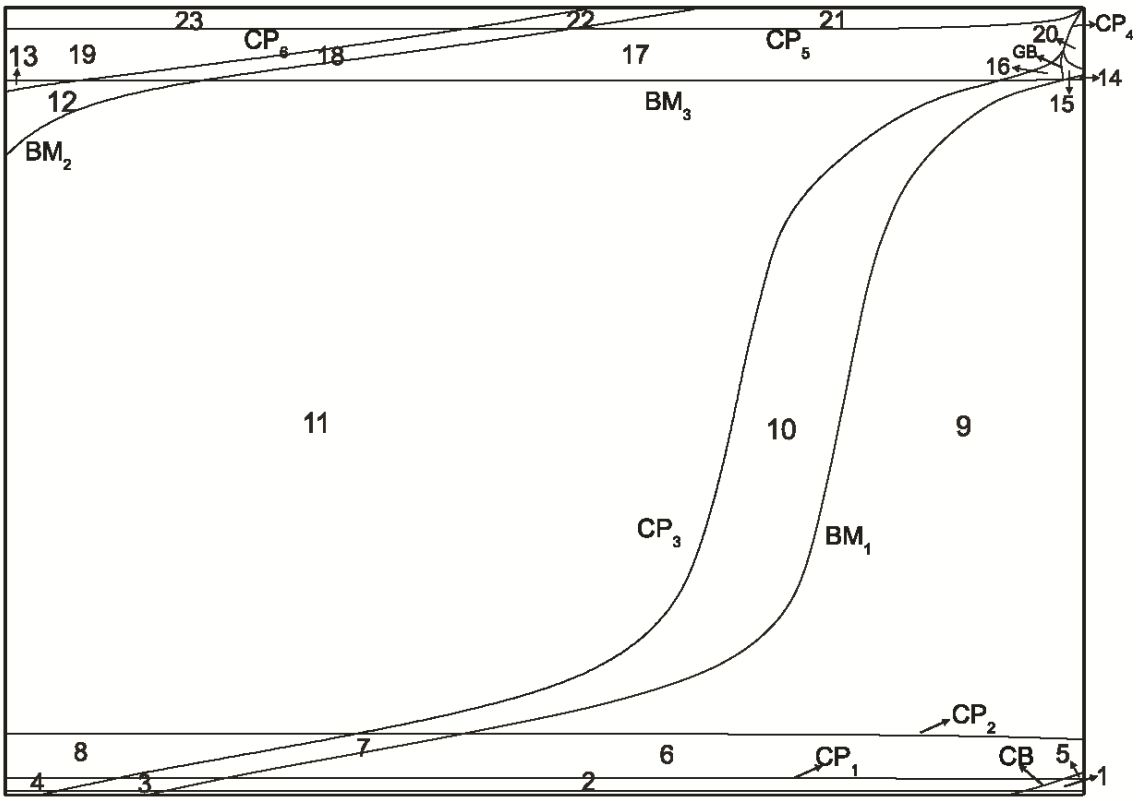

Figure 5. (h_1, h_2) control space diagram for the cavity. The numbers in each region refer to flow strustures in Figure 2, Figure 3 and Figure 4.

4. THE MECHANISM OF EDDY GENERATION WITHIN THE DOMAIN

Four types of bifurcation are observed in parameter space (h_1, h_2). The first type of bifurcation appears on the wall at which two on-wall saddle points come together to form an off-wall saddle point. The curves representing this bifurcation in the diagram are called BM. In the second type of bifurcation, the degenerate points are transformed from the saddle into the centre point inside the flow such that it is called cusp bifurcation and denoted by CP in the parameter space. These types of degenerate critical points are illustrated in Figure 6. In the global bifurcation which is named by GB, there is a change in the flow structure but no change in the number of critical points. In the last type, the center point transform into saddle and vice versa. This type of bifurcation is named by CB.

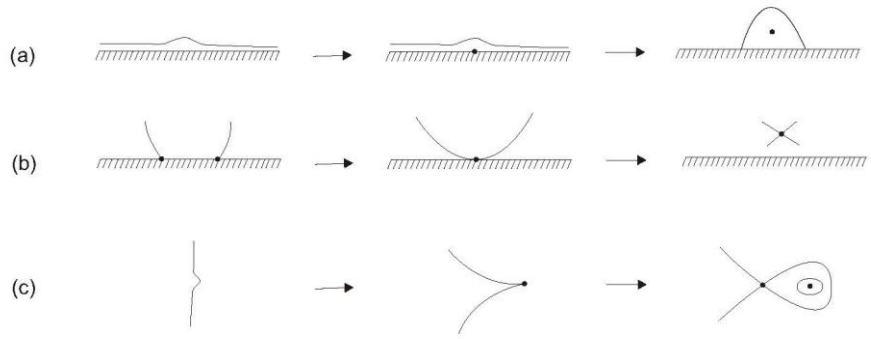

Figure 6. Streamline topology near a stationary wall (a)-(b) and away from boundary (c).

A mechanism of flow transformation according to varying the heights of the lower part and upper part of the cavity is given in Figure 2, Figure 3 and Figure 4. When the upper part of the cavity is small, for example $0.2 < h_2 < 1.0$, the discontinuity of the stream lines causes the flow structure not to be fully understood. In this case, the bi-section method given by Gaskell [21] is used to understand whether the critical point is a saddle or centre. In this study, the vertical velocity decided the type of structures near the critical point, depending on the sign exchange in the vector component. A similar approach is used in this study in regions 1-8 in Figure 2.

Below the curve of the CP_1, there is a flow pattern giving rise to a separatrix enclosing the five sub-eddies at the upper part of the cavity and two corner eddies at the lower part. In the flow structure illustrated in Figure 2(1), the main vortex of separatrix contains 2 separatrices nested within the central section. When we cross to the second region by CB curve, the saddle critical point at the central section of the first structure is transformed into the centre critical point. When h_2 is constant and the h_1 is decreased, the formation of the second vortex in the lower part of the cavity occurs by the known vortex formation mechanism, as shown in Figure 2 ($2 \rightarrow 3 \rightarrow 4$). This mechanism was observed in the square cavity by Gürcan [19] and in the L-shaped cavity by Deliceoğlu [26] for the S = 0. There is also a similar flow transformation series between the CP_1 and CP_2, Figure 2($6 \rightarrow 7 \rightarrow 8$), or CP_2 and BM_3 curve, Figure 2-Figure3 ($9 \rightarrow 10 \rightarrow 11$). While this series occurs, the separation line that separates the lower cavity and the upper cavity moves upward. However, the saddle-node bifurcation, where the corners of the upper cavity and the separation line coalesce, occurs at the same value of h_1.

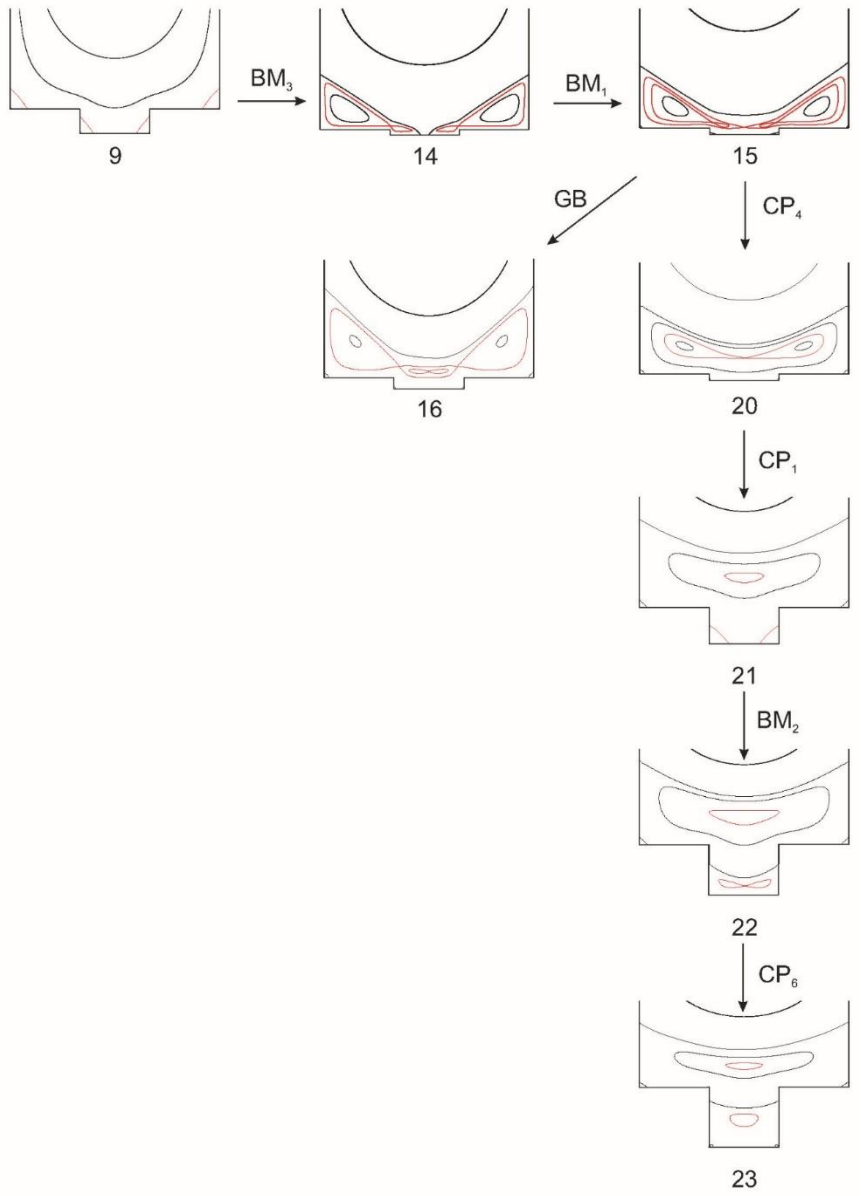

Figure 7. The mechanism of eddy generation via several transformation which is similar with in the rectangular cavity.

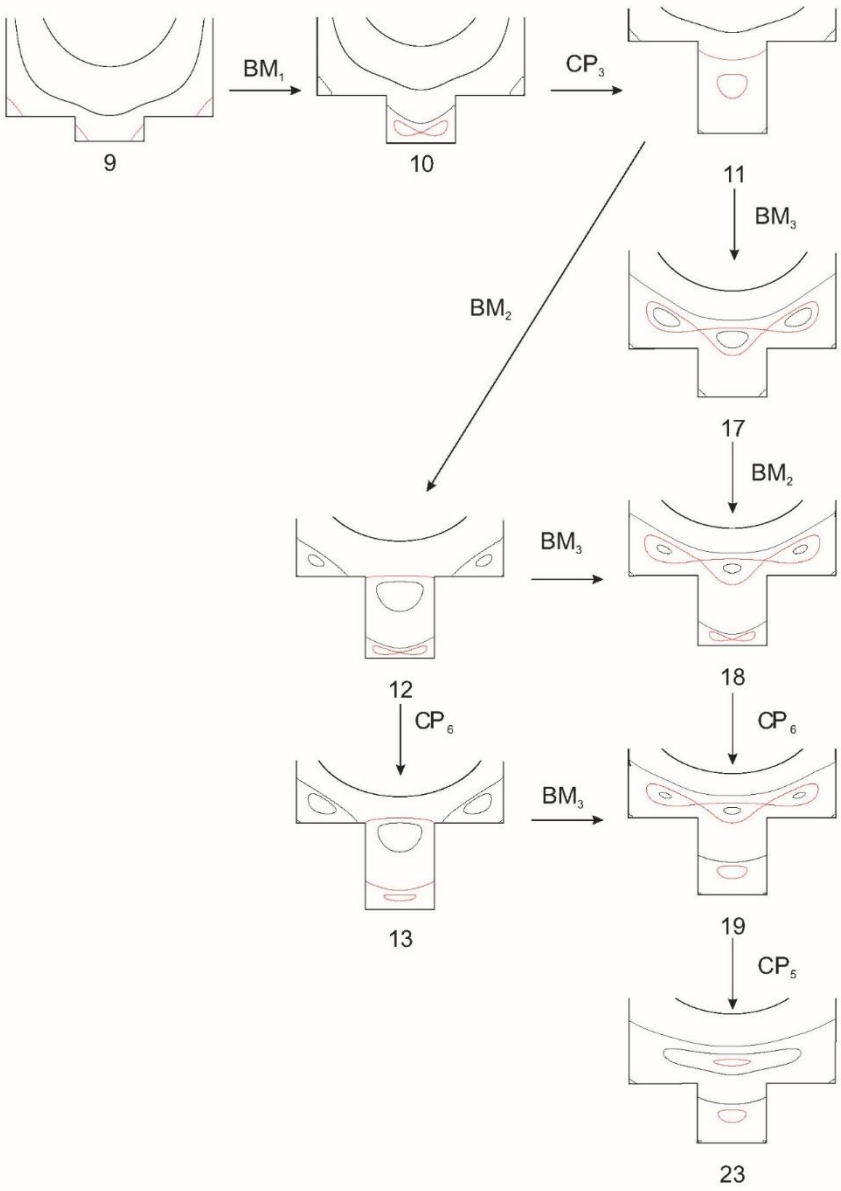

Figure 8. The series of bifurcation which is previously unseen.

Another vortex formation scenario is seen when the lower cavity height is sufficiently small. The corner vortices of the lower cavity coalesce with the corner vortices of the upper cavity before they are joined together. Thus, there are two corner vortices containing separatrix inside the cavity. After BM and CP bifurcation, separatrix is formed inside the fluid as in the square cavity and after the CP bifurcation, the second vortex is formed as in Figure 7 ($9 \rightarrow 14 \rightarrow 15 \rightarrow 20 \rightarrow 21$). There are a few basic scenarios for the new vortex formation, where the separation line crosses the corner point and is coalesced with the corner vortices. These different flow transformation scenarios are shown in Figure 8.

5. CONCLUSION

In this study, we have shown the flow patterns and eddy generation in a T-shaped cavity. The flow is generated by the motion of the upper lid of the cavity. The (h_1, h_2) control space diagram have obtained for the interval between $-3.5 < h_1 < -0.2$ and $0.2 < h_2 < 10.5$. It is observed that the bifurcation transformation series in order to increase the number of eddies in the lower cavity is the same as in the square cavity as h_2 is constant. Furthermore, when h_1 was sufficiently small, it is observed for the first

time that the vortex formation occurred by joining the corner vortices together. In other cases, the number of vortices within the cavity increases as a result of various bifurcations series of the dividing line with corner vortices.

REFERENCES

[1] Shankar, P. N., The eddy structure in Stokes flow in a cavity, Journal of Fluid Mechanics, 250 (1993) 371–383.

[2] Gaskell, P. H., Gürcan, F., Savage, M. D., Thompson, H. M., Stokes flow in a double-lid-driven cavity with free surface side walls, Proceedings of the Institution of Mechanical Engineers, Part C: Journal of Mechanical Engineering Science, 212(5) (1998) 387–403.

[3] Gürcan, F., Gaskell, P. H., Savage, M. D., Wilson, M. C. T., Eddy genesis and transformation of Stokes flow in a double-lid driven cavity, Proceedings of the Institution of Mechanical Engineers, Part C: Journal of Mechanical Engineering Science, 217(3) (2003) 353–364.

[4] Liu, C., Joseph, D., Stokes flow in wedge-shaped trenches, Journal of Fluid Mechanics, 80(3) (1977) 443-463.

[5] R Schreiber, H.B Keller, Driven cavity flows by efficient numerical techniques, Journal of Computational Physics, 49(2) (1983) 310-333.

[6] Erturk, E., Gokcol, O., Fine Grid Numerical Solutions of Triangular Cavity Flow, Applied Physics, 38(1) (2007) 97–105.

[7] Deliceoğlu, A., Aydin, S. H. Topological flow structures in an L-shaped cavity with horizontal motion of the upper lid, Journal of Computational and Applied Mathematics, 259(PART B) (2014) 937–943.

[8] Gürcan, F., Bilgil, H., Bifurcations and eddy genesis of Stokes flow within a sectorial cavity, European Journal of Mechanics, B/Fluids, 39 (2013) 42-51.

[9] Brøns, M., Hartnack, J. N., Streamline topologies near simple degenerate critical points in two-dimensional flow away from boundaries, Physics of Fluids, 11(2) (1999) 314–324.

[10] Gürcan, F., Deliceoğlu, A., Bakker, P. G., Streamline topologies near a non-simple degenerate critical point close to a stationary wall using normal forms, Journal of Fluid Mechanics, 539 (2005) 299–311.

[11] Gürcan, F., Deliceoğlu, A., Streamline topologies near non-simple degenerate points in two-dimensional flows with double symmetry away from boundaries and an application, Physics of Fluids, 17(9) (2005) 1–7.

[12] Hartnack, J. N., Streamlines topologies near a fixed wall using normal forms, Acta Mechanica, 75 (1999) 55–75.

[13] Erturk, E., Corke, T. C. and Gökçöl, C., Numerical solutions of 2-D steady incompressible driven cavity flow at high Reynolds numbers. Int. J. Numer. Meth. Fluids, 48 (2005) 747-774.

[14] Botella, O., Peyret, R., Benchmark Spectral Results on the Lid Driven Cavity Flow, Computers and Fluids, 27(4) (1998) 421–433.

[15] Driesen, CH, Kuerten, JGM and Streng, M., Low-Reynols-Number flow over partially covered cavities, J. Eng. Math., 34 (1998) 3-20.

[16] Gaskell, PH, Savage, MD, Summers, JL and Thompson, HM., Stokes flow in closed, rectangular domains, Applied Mathematical Modelling, 22 (1998) 727-743.

[17] Ghia, U, Ghia, KN and Shin, CT., High-Re solution for incompressible flow using the Navier-Stokes equations and a multigrid method, J. Comp. Physics, 48 (1982) 387-411.

[18] Gürcan, F., Effect of the Reynolds number on streamline bifurcations in a double-lid-driven cavity with free surfaces, Computers and Fluids, 32 (2003) 1283-1298.

[19] Gürcan, F., Flow bifurcations in rectangular, lid-driven, cavity flows. PhD. Thesis (1996), University of Leeds.

[20] William D. McQuain, Calvin J. Ribbens, C.-Y. Wang, Layne T. Watson., Steady viscous flow in a trapezoidal cavity, Computers and Fluids, 23(4) (1994) 613-626.

[21] Gaskell, P., Savage, M., Wilson, M., Stokes flow in a half-filled annulus between rotating coaxial cylinders, Journal of Fluid Mechanics, 337 (1997) 263-282.

[22] Ribbens, C. J., Watson, L. T., Wang, C.-Y., Steady Viscous Flow in a Triangular Cavity, Journal of Computational Physics, 112(1) (1994) 173–181.

[23] Gaskell, P.H., Thompson, H, Savage, M., A finite element analysis of steady viscous flow in triangular cavities, Proceedings of The Institution of Mechanical Engineers Part C-journal of Mechanical Engineering Science, 213 (1999) 263-276.

[24] Gurcan, F., Bilgil, H., Bifurcations and eddy genesis of Stokes flow within a sectorial cavity PART II: Co-moving lids, European Journal of Mechanics- B/Fluids, 56 (2015) 42–51.

[25] Bilgil, H., Gürcan, F., Effect of the Reynolds number on flow bifurcations and eddy genesis in a lid-driven sectorial cavity, Japan Journal of Industrial and Applied Mathematics, 33(2) (2016) 343–360.

[26] Deliceoğlu, A., Aydin, S. H., Flow bifurcation and eddy genesis in an L-shaped cavity, Computers and Fluids, 73 (2013) 24-46.

[27] E.B. Becker, G.F. Carey and J.T. Oden, Finite Elements, An introduction Vol. I. Prentice-Hall, 1981, New Jersey.

[28] Aydın, S. H., The Finite Element Method Over a Simple Stabilizing Grid Applied to Fluid Flow Problems, PhD Thesis (2008).